

mation as well as the importance of the Coulomb excitation process. Professor G. H. Rawitscher and Professor J. S. McIntosh also have discussed with us the theoretical interpretation of the data. The experimental portion of this work has been greatly assisted by the work of J. Shuchatowitz on the evaporation of

targets, K. Chung on the improvement of the resolution of the scintillation counter, A. Disco and J. Gill on the angle indicator, and D. Bates on the target positioning control. Finally, we wish to thank the accelerator crew under the direction of Dr. M. S. Malkin for the necessary heavy-ion beams.

PHYSICAL REVIEW

VOLUME 125, NUMBER 2

JANUARY 15, 1962

## Gamma Radiation from Proton Capture in $\text{Na}^{23}\dagger$

F. W. PROSSER, JR., W. P. UNRUH, B. H. WILDENTHAL, AND R. W. KRONE

*The University of Kansas, Lawrence, Kansas*

(Received September 11, 1961)

The  $\gamma$ -ray decays of twelve resonances in the reaction  $\text{Na}^{23}(p,\gamma)\text{Mg}^{24}$  in the proton energy range from 0.58 to 1.42 Mev have been re-examined with large scintillation detectors and coincidence techniques. A number of weaker cascades through the states of  $\text{Mg}^{24}$  between the excitation energies of 6 Mev and 8 Mev has been found. Relative intensities have been measured for the observed  $\gamma$  rays and consistent decay schemes proposed. The absolute yields of this reaction at these resonances have been determined.

### INTRODUCTION

INCREASING interest in the collective interpretation of nuclear states in the nuclei of the  $d_{5/2}$  shell<sup>1,2</sup> has prompted several recent investigations<sup>3-5</sup> of the states of  $\text{Mg}^{24}$ . A number of the states of intermediate excitation in  $\text{Mg}^{24}$  also are reached in the decay of various compound states observed in the  $\text{Na}^{23}(p,\gamma)\text{Mg}^{24}$  reaction. Since most of the information on this reaction was obtained several years ago,<sup>6-10</sup> it was felt that a more thorough study, with the use of the multichannel analyzers and the larger scintillation crystals now available, would be of value. This paper will be primarily concerned with the assignment of relative intensities to the various  $\gamma$  rays observed and their incorporation into decay schemes at the resonances in this reaction between the bombarding energies of 0.58 and 1.42 Mev. Also, the absolute yield for  $\gamma$ -ray decay,  $\omega\gamma$ , of these resonances has been measured. The angular distribu-

tions and correlations of several of these  $\gamma$  rays will be discussed in a subsequent paper.

### EXPERIMENTAL PROCEDURE

The electronics used in this study were standard. The  $\gamma$  radiation was detected with a 5-in. diam $\times$ 5-in. thick NaI crystal mounted on a DuMont 6263 photomultiplier tube and the resulting pulse-height distributions were recorded on an RCL 256-channel analyzer. Where the complexity of the pulse height spectra required coincidence studies for confirmation of the proposed cascades, a 3-in. diam $\times$ 3-in. thick NaI crystal was used as the second detector in a slow-fast coincidence circuit. The fast coincidence circuit consisted of four Hewlett-Packard Model 460AR amplifiers and an E-H Research Laboratories Model 101N coincidence analyzer with the resolving time set at 25 nsec. A slow coincidence between the fast-coincidence output and a window set on the desired portion of the spectrum from the 5-in. $\times$ 5-in. detector gated the multichannel analyzer.

For most of the work and for the final assignment of relative intensities, the spectra were observed at an angle of  $55^\circ$  to the incident beam to minimize the effect of angular distributions on these assignments. To improve the effective resolution of the pulse height spectra, a 3-in. thick lead collimator was inserted between the target and the detector. The opening in the collimator was tapered to permit the passage of  $\gamma$  rays only in a cone which traversed the entire crystal. For the coincidence studies, the 5-in. $\times$ 5-in. crystal was left at  $55^\circ$  with the collimator in place and the 3-in. $\times$ 3-in. crystal was placed at about  $80^\circ$  to the beam on the opposite side of the target with its front face one inch from the target.

The targets were prepared by the evaporation of

$\dagger$  This work has been supported in part by the U. S. Atomic Energy Commission.

<sup>1</sup> H. E. Gove, *Proceedings of the International Conference on Nuclear Structure, Kingston*, edited by D. A. Bromley and E. W. Vogt (University of Toronto Press, Toronto, 1960), pp. 438-460.

<sup>2</sup> M. K. Banerjee, reference 1, pp. 461-463.

<sup>3</sup> C. Broude and H. E. Gove, reference 1, pp. 471-474.

<sup>4</sup> R. Batchelor, A. J. Ferguson, H. E. Gove, and A. E. Litherland, *Nuclear Phys.* **16**, 38 (1960).

<sup>5</sup> E. W. Hamburger and A. G. Blair, *Phys. Rev.* **119**, 777 (1960).

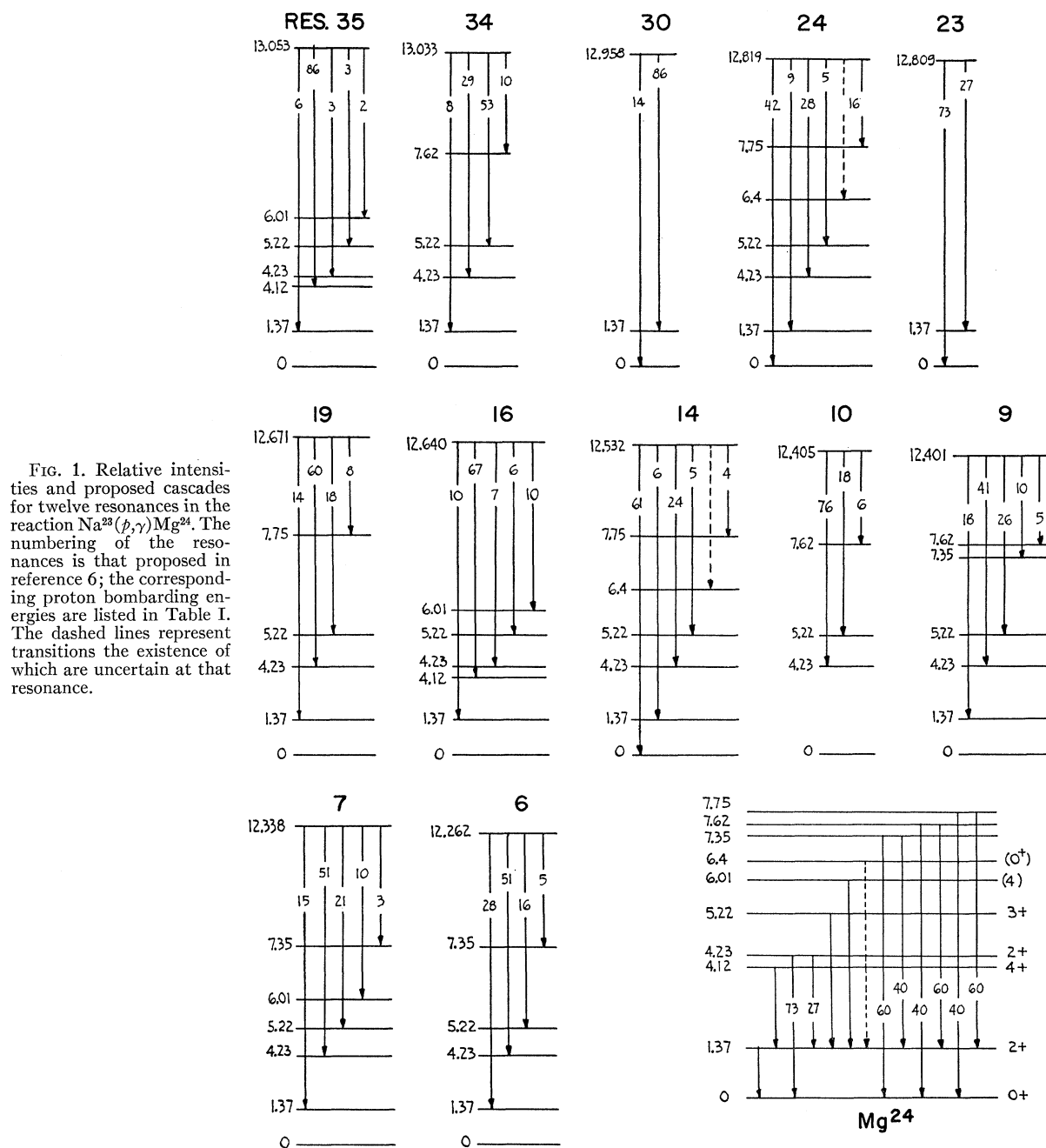
<sup>6</sup> F. W. Prosser, Jr., N. B. Baumann, D. K. Brice, W. G. Read, and R. W. Krone, *Phys. Rev.* **104**, 369 (1956).

<sup>7</sup> J. O. Newton, *Phys. Rev.* **96**, 241 (1954).

<sup>8</sup> F. C. Flack, J. G. Rutherglen, and P. J. Grant, *Proc. Phys. Soc. (London)* **A67**, 973 (1954).

<sup>9</sup> P. J. Grant, J. G. Rutherglen, F. C. Flack, and G. W. Hutchinson, *Proc. Phys. Soc. (London)* **A68**, 369 (1955).

<sup>10</sup> For a general bibliography of other reactions leading to  $\text{Mg}^{24}$ , see P. M. Endt and C. M. Braams, *Revs. Modern Phys.* **29**, 683 (1957), and *Nuclear Data Sheets* (National Academy of Sciences-National Research Council, Washington, D. C., 1960).



$\text{Na}_2\text{SO}_4$  onto Au backings. The use of these targets in conjunction with liquid nitrogen cold trapping immediately adjacent to the target and a diffusion pump vacuum maintained at the target minimized the problem of  $\text{F}^{19}$  contamination of the target, a difficulty which plagued the earlier work. Very little deterioration of these targets was noticed even after extensive bombardment. Some carbon buildup did occur but was not detrimental to the present work. For some of the earlier work, similar targets were prepared with  $\text{NaCl}$ . These were equally satisfactory in most respects, but the pulse

height distributions at several resonances showed weak lines from proton capture in the  $\text{Cl}$  which tended to mask interesting details in the  $\text{Mg}^{24}$  decay.

## EXPERIMENTAL RESULTS

### I. Relative Intensities and Cascades

The energy calibration for each pulse height spectrum was determined from the prominent, known  $\gamma$  rays in the spectrum itself. This method resulted in a consistent and reproducible calibration which allowed the identi-

fication of all structure evident in the original spectra to an accuracy of  $\pm 50$  kev. The pulse height shapes associated with monochromatic  $\gamma$  rays were determined by the observation of the well separated or essentially monochromatic  $\gamma$  rays from the reactions  $B^{11}(p,\gamma)C^{12}$ ,  $C^{13}(p,\gamma)N^{14}$ , and  $F^{19}(p,\alpha\gamma)O^{16}$ , with the target and detector geometry the same as that used for the experiment. The results for each resonance will be discussed separately and, for convenience, the resonances will be referred to with the numbering used in reference 6. The results for all resonances are summarized in Fig. 1 and Table I. The analyzed beam current available at the target was limited to a maximum of  $10 \mu\text{amp}$ . This made the observation of  $\gamma$  rays with an intensity of less than a few percent of those in the dominant cascades difficult and subject to some error. This, of course, was particularly true where these weak  $\gamma$  rays were at energies close to those in the strong cascades, which prevented unambiguous separation even by coincidence techniques. No uniform attempt was made, therefore, to identify these weaker decays.

#### Resonance 35

This decay is dominated by the cascade through the  $4+$ , 4.12-Mev state, as indicated in Table I. Even though no coincidence measurements were attempted at this resonance, it is felt that the 4.6-Mev  $\gamma$  ray is probably the result of the transition from the state at 6.01 Mev, tentively identified as also having spin  $4$ .<sup>8</sup> However the required transition to the 6.01-Mev state could not be distinguished with certainty.

#### Resonance 34

The decay of this resonance is somewhat more complex, as shown by the pulse height spectrum in Fig. 2, and coincidence measurements were carried out to identify the  $\gamma$  rays of 5.40 and 6.27 Mev. The pulse

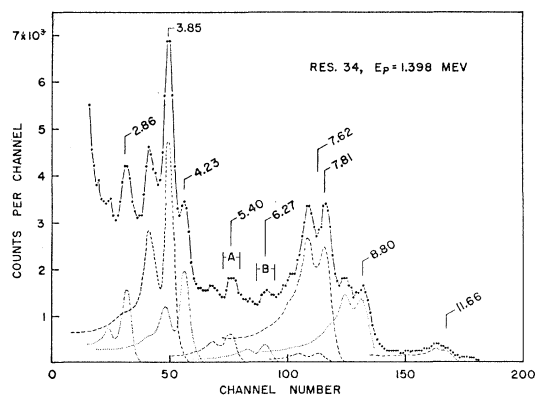


FIG. 2. Pulse height spectrum obtained with the 5-in. $\times$ 5-in. crystal at resonance 34. The points connected by solid lines are the original data, while the dotted and dashed lines represent the  $\gamma$  rays believed to be present in the spectrum. The bracketed regions *A* and *B* are the windows used in the coincidence measurements. The background is negligible over this portion of the spectrum.

TABLE I. Relative intensities of the  $\gamma$  rays observed at the resonances in the  $Na^{23}(p,\gamma)Mg^{24}$  reaction. The relative intensities, with their standard errors, are given parenthetically following the energies of the  $\gamma$  rays and are in arbitrary units based on 100 for the strongest high-energy  $\gamma$  ray in the spectrum. The energies of the  $\gamma$  rays whose presence in the spectra are less certain or which were not fitted into a decay scheme are shown in italics.

Resonance	Proton energy (kev)	Excitation energy (Mev)	$\gamma$ -ray energy (Mev) and relative intensity
6	594	12.262	10.89 (56 $\pm$ 5); 8.03 (100 $\pm$ 5); 7.04 (32 $\pm$ 5); 6.05 (9 $\pm$ 2); 4.90 (8 $\pm$ 2); 4.23 (80 $\pm$ 4); 3.85 (46 $\pm$ 4); 2.86 (31 $\pm$ 6); 1.37 (144 $\pm$ 20)
7	675	12.338	10.97 (30 $\pm$ 4); 8.80 (4 $\pm$ 2); 8.10 (100 $\pm$ 8); 7.35 (13 $\pm$ 5); 7.11 (41 $\pm$ 7); 6.32 (11 $\pm$ 4); 5.98 (15 $\pm$ 4); 4.98 (19 $\pm$ 4); 4.64 (6 $\pm$ 3); 4.23 (76 $\pm$ 4); 3.85 (40 $\pm$ 4); 2.86 (30 $\pm$ 4); 1.37 (120 $\pm$ 4)
9	740	12.401	11.03 (42 $\pm$ 5); 9.2 (20 $\pm$ 6); 8.8 (13 $\pm$ 4); 8.17 (100 $\pm$ 5); 7.62 (13 $\pm$ 6); 7.35 (27 $\pm$ 8); 7.18 (64 $\pm$ 8); 6.30 (10 $\pm$ 4); 5.98 (13 $\pm$ 5); 5.05 (23 $\pm$ 4); 4.78 (13 $\pm$ 4); 4.23 (84 $\pm$ 6); 3.85 (48 $\pm$ 6); 2.86 (38 $\pm$ 6); 1.37 (120 $\pm$ 15)
10	744	12.405	8.18 (100 $\pm$ 3); 7.18 (24 $\pm$ 4); 6.29 (7 $\pm$ 3); 4.75 (8 $\pm$ 3); 4.23 (78 $\pm$ 5); 3.85 (22 $\pm$ 4); 2.86 (27 $\pm$ 5); 1.37 (49 $\pm$ 7)
14	877 <sup>a</sup>	12.532	12.53 (100 $\pm$ 3); 11.16 (11 $\pm$ 2); 9.3 (2 $\pm$ 1); 8.30 (39 $\pm$ 2); 7.72 (5 $\pm$ 2); 7.31 (8 $\pm$ 4); 6.30 (5 $\pm$ 3); 6.00 (4 $\pm$ 2); 5.00 (4 $\pm$ 2); 4.80 (7 $\pm$ 3); 4.23 (31 $\pm$ 4); 3.85 (11 $\pm$ 3); 2.86 (9 $\pm$ 3); 1.37 (44 $\pm$ 8)
16	989	12.640	11.27 (13 $\pm$ 3); 9.4 (5 $\pm$ 2); 8.52 (100 $\pm$ 4); 7.45 (7 $\pm$ 2); 6.60 (13 $\pm$ 2); 4.62 (12 $\pm$ 2); 4.23 (8 $\pm$ 2); 3.85 (10 $\pm$ 2); 2.75 (84 $\pm$ 4); 1.37 (110 $\pm$ 10)
19	1022	12.671	11.30 (24 $\pm$ 3); 8.44 (100 $\pm$ 4); 7.45 (30 $\pm$ 4); 6.35 (6 $\pm$ 2); 4.94 (14 $\pm$ 3); 4.23 (85 $\pm$ 5); 3.85 (29 $\pm$ 4); 2.86 (25 $\pm$ 3); 1.37 (94 $\pm$ 10)
23	1166	12.809	12.81 (100 $\pm$ 10); 11.44 (37 $\pm$ 7)
24	1176	12.819	12.82 (100 $\pm$ 10); 11.44 (21 $\pm$ 4); 9.4 (12 $\pm$ 4); 8.58 (66 $\pm$ 5); 7.75 (13 $\pm$ 6); 7.60 (13 $\pm$ 6); 6.40 (37 $\pm$ 7); 5.05 (38 $\pm$ 7); 4.23 (70 $\pm$ 20); 3.85 (12 $\pm$ 5); 2.86 (25 $\pm$ 8); 1.37 (94 $\pm$ 15)
30	1321	12.958	12.96 (16 $\pm$ 3); 11.59 (100 $\pm$ 4); 1.37 (93 $\pm$ 5)
34	1398	13.033	11.66 (14 $\pm$ 2); 8.80 (55 $\pm$ 4); 7.81 (100 $\pm$ 8); 7.6 (6 $\pm$ 3); 6.27 (11 $\pm$ 3); 5.40 (19 $\pm$ 4); 4.23 (42 $\pm$ 5); 3.86 (99 $\pm$ 8); 2.86 (27 $\pm$ 5); 1.37 (160 $\pm$ 16)
35	1419	13.053	11.68 (7 $\pm$ 2); 10.1 (4 $\pm$ 2); 8.93 (100 $\pm$ 3); 4.60 (2 $\pm$ 1); 4.23 (4 $\pm$ 1); 3.85 (3 $\pm$ 1); 2.75 (100 $\pm$ 3); 1.37 (112 $\pm$ 5)

<sup>a</sup> This resonance has been assigned energies from 869 kev to 877 kev in various studies. Using a thin target deliberately contaminated with  $F^{19}$ , we find that the resonance is  $1.4 \pm 0.4$  kev above the strong resonance in the  $F^{19}(p,\alpha\gamma)O^{16}$  reaction.

height distribution and coincidence spectra obtained with the 3-in.  $\times$  3-in. crystal are shown in Fig. 3. It is clear, from the spectrum obtained in coincidence with window *B* in Fig. 2, that the 6.27-Mev  $\gamma$  ray is in coincidence with the 5.40- and 1.37-Mev  $\gamma$  rays. From the spectrum obtained in coincidence with window *A*, a weak indication of a 7.6-Mev  $\gamma$  ray is evident, in addition to those of 6.27 and 1.37 Mev. This is in agreement with the decay of the 7.62-Mev state in  $\text{Mg}^{24}$  as observed by Glaudemans.<sup>11</sup> The identification of the other  $\gamma$  rays is straightforward and is indicated in Fig. 1. The small departure of the intensity ratio from the accepted value<sup>4</sup> of about 26 to 74 for the 2.87 and 4.23-Mev  $\gamma$  rays from the decay of the 4.23-Mev state may result from a small admixture of the decay through the 4.12-Mev state.

### Resonance 30

As indicated by the results shown in Fig. 1 and Table I, the decay of this state is quite simple. There is some evidence for alternate cascades in the pulse height spectrum, but they are too weak to identify with any certainty. None appear to have an intensity greater than one percent of the 11.58-Mev  $\gamma$  ray. The relatively strong ground-state transition casts doubt on the assignment of  $3+$  to the compound state given in reference 6, which was based on the presence of  $\cos^4\theta$  terms in the angular distribution together with the assumption that the state would be formed by the lowest possible orbital angular momentum.

### Resonance 24

At this resonance the spectrum, shown in Fig. 4, is again complex and required coincidence measurements for confirmation of the proposed decay scheme. The coincidence spectra in Fig. 5 show clearly that the 5.05-Mev  $\gamma$  ray is in coincidence with both the 6.40- and 1.37-Mev  $\gamma$  rays, as well as with the much weaker 7.7-Mev  $\gamma$  ray. This is in essential agreement with the decay of the 7.75-Mev state observed by Glaudemans.<sup>11</sup> However, the presence of a strong transition to the  $0+$  ground state and the fact that the 6.40-Mev  $\gamma$  ray appears much stronger relative to the 7.7-Mev  $\gamma$  ray than reported in reference 11 suggest that part of the 6.40–5.05–1.37 cascade proceeds by way of the state at 6.4 Mev seen by Broude and Gove<sup>3</sup> and reported by them to be also a state of spin 0.

### Resonance 23

This resonance shows much the same pulse height spectrum that was seen at resonance 30, except that the ground-state transition is relatively stronger. Stelson<sup>12</sup> has assigned spin and parity  $2+$  to this resonance on the basis of the isotropic angular distribution of the  $\alpha$

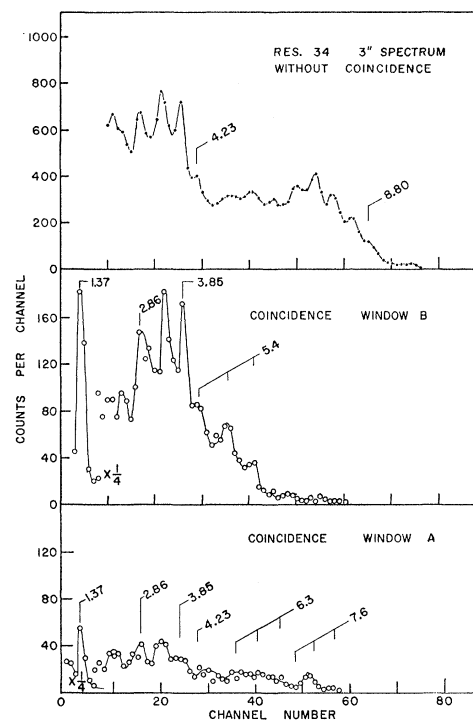


FIG. 3. Coincidence spectra obtained at resonance 34 with the 3-in.  $\times$  3-in. crystal. The sample spectrum shown at the top was taken to establish the energy scale and to identify the structure in the coincidence spectra. The lower two spectra were obtained in coincidence with the windows indicated in Fig. 2.

particles in the  $\text{Na}^{23}(p,\alpha)\text{Ne}^{20}$  reaction and this assignment was tentatively confirmed on the basis of the proton elastic scattering data by Baumann *et al.*<sup>13</sup> In view of the  $\gamma$ -ray decay of the state, however, the assignment of  $1-$  given by Newton<sup>7</sup> appears to be equally plausible and is not inconsistent with the angular distribution of the  $\alpha$  particles if the state is formed primarily from channel spin 2. It is hoped that measurement of the angular correlation of the capture  $\gamma$  rays in the cascade through the 1.37-Mev state or of the  $\alpha$  particles and  $\gamma$  rays in the  $\text{Na}^{23}(p,\alpha\gamma)\text{Ne}^{20}$  reaction will enable a clear choice to be made. The relative intensity of the 1.37-Mev  $\gamma$  ray could not be measured at this resonance because of the intense 1.63-Mev radiation from the  $\text{Na}^{23}(p,\alpha\gamma)\text{Ne}^{20}$  reaction.

### Resonance 19

Other than for changes in the intensity ratios, the decay of this state appears quite similar to that of resonance 34. Weak  $\gamma$  rays of 4.94 and 6.35 Mev are present and, although no coincidence measurements were attempted for confirmation, are undoubtedly the result of a cascade through the state at 7.75 Mev seen also at resonance 24. The corresponding weak  $\gamma$  ray of 7.75 Mev is, of course, completely masked by the much

<sup>11</sup> P. W. M. Glaudemans, quoted by P. M. Endt, *Nuclear Instr. and Methods* **11**, 3 (1961).

<sup>12</sup> P. H. Stelson, *Phys. Rev.* **96**, 1584 (1954).

<sup>13</sup> N. B. Baumann, F. W. Prosser, Jr., W. G. Read, and R. W. Krone, *Phys. Rev.* **104**, 376 (1956).

stronger 8.43- and 7.43-Mev transitions to the 4.23- and 5.22-Mev states, respectively.

### Resonance 16

This decay is similar, except for altered intensity ratios, to that seen at resonance 35. In particular, the cascade through the 6.01-Mev state is seen in considerably greater intensity. The much weaker  $\gamma$  ray seen at 9.8 Mev was not fitted into the decay scheme.

### Resonance 14

The pulse height distribution obtained at resonance 14 is shown in Fig. 6. In addition to the transitions to the ground and first excited states previously reported,<sup>7</sup> the virtual absence of  $F^{19}$  contamination of the target allows transitions to a number of intermediate states to be seen. A weak decay through the 7.75-Mev state is evident, and the very weak structure at 5.05 Mev suggests a decay through the 6.4-Mev state. No attempt was made to assign the  $\gamma$  ray seen at about 9.3 Mev to a cascade.

### Resonance 10

At this resonance the results were in essential agreement with those reported in reference 11. However, the absence of any observed structure at 8.7 Mev leads us to the conclusion that the  $\gamma$  rays observed at 3.82 and 7.23 Mev are associated with a cascade through the 5.22-Mev state. This interpretation is strengthened by the fact that at all other resonances at which decay occurs to the 4.23-Mev state there is also a branch to the 5.22-Mev state. An alternate interpretation which would explain the slight discrepancy in energy observed from those required for the postulated transitions as well as the apparent absence of the 8.7-Mev  $\gamma$  ray in our spectrum

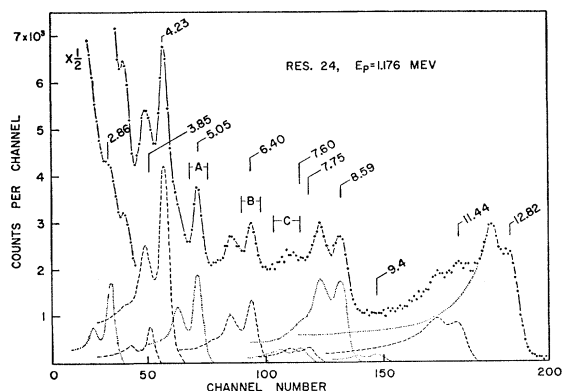


FIG. 4. Pulse height spectrum obtained with the 5-in.  $\times$  5-in. crystal at resonance 24. The points connected by solid lines are the original data, while the dotted and dashed lines represent the  $\gamma$  rays believed to be present in the spectrum. The bracketed regions A, B, and C are the windows used in the coincidence measurements. The background is negligible over this portion of the spectrum.

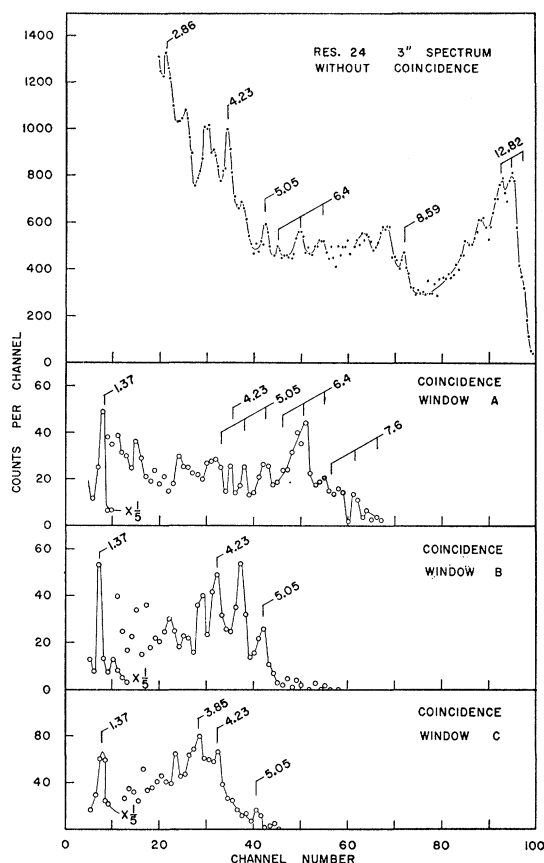


Fig. 5. Coincidence spectra obtained at resonance 24 with the 3-in.  $\times$  3-in. crystal. The sample spectrum shown at the top was taken to establish the energy scale and to identify the structure in the coincidence spectra. The lower three spectra were obtained in coincidence with the windows indicated in Fig. 4.

would be that both cascades are present in about equal intensities.

### Resonances 6, 7, and 9

Except for the differences in relative intensities, the results obtained at these resonances are in agreement with those reported by Glaudemans.<sup>11</sup> Also, as mentioned above, the current limitations of the Van de Graaff accelerator precluded investigation of the much weaker transitions<sup>11</sup> through the high-energy intermediate states.

## II. Absolute Yields

The yields were determined from the excitation curve obtained at each resonance with the 5-in.  $\times$  5-in. detector. The detector was placed at  $55^\circ$  and the  $\gamma$  rays were collimated, as described above. The target used for all resonances, except resonance 6, was prepared by evaporation of  $Na_2SO_4$  and was determined to be about 12-kev thick at resonance 35. For resonance 6, the target was  $NaCl$  and the yield obtained was corrected to that of the  $Na_2SO_4$  target by comparison with the yield obtained

TABLE II. Absolute yields of the reaction  $\text{Na}^{23}(p,\gamma)\text{Mg}^{24}$ . The thick target yields are those for an evaporated target of  $\text{Na}_2\text{SO}_4$ . The assumptions used in the calculation of  $(2J+1)\Gamma_\gamma$  are discussed in the text.

Resonance	Thick-target yield ( $\gamma$ 's/proton $\times 10^{11}$ )	$\omega\gamma$ (ev)	$(2J+1)\Gamma_\gamma$ (ev)
6	5.4	0.21	1.9
7	16.6	0.70	5.6
9	3.7	0.16	1.3
10	4.6	0.20	1.6
14	12.1	0.58	5.1
16	5.9	0.29	2.4
19	45.2	2.3	20
23	5.3	0.28	4.4 <sup>a</sup>
24	28.4	1.5	17
30	146	7.9	63
34	34.7	1.9	22
35	92.5	5.1	81 <sup>a</sup>

<sup>a</sup>  $\Gamma_p$  assumed to be  $0.5\Gamma$ .

with the NaCl target at resonance 7. The target was checked for deterioration periodically, but no change other than a small shift in energy from carbon deposition was found. The yield obtained at each resonance was corrected, on the basis of the pulse height spectrum obtained at that resonance, for the presence of more than one  $\gamma$  ray in some of the cascades above the discriminator bias used at that resonance. The thin target yields were then changed to the equivalent infinite target yields.<sup>14</sup> The proton current was monitored with a standard current integrator which was calibrated at a standard current approximately equal to the beam current used in the yield determinations. The yields were finally corrected for detector efficiency and solid angle, with the assumption of isotropy, and are shown in Table II. These yields are assigned a standard error of  $\pm 15\%$ , the primary uncertainty arising from the correction for the pulse height distributions.

<sup>14</sup> H. E. Gove, *Nuclear Reactions*, edited by P. M. Endt and M. Demeur (North-Holland Publishing Company, Amsterdam, 1959), Vol. I, Chap. VI, pp. 259-317.

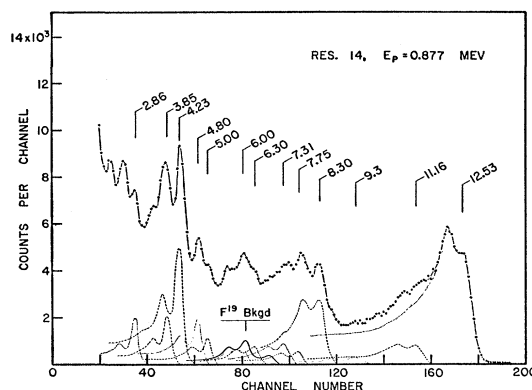


Fig. 6. Pulse height spectrum obtained with the 5-in.  $\times$  5-in. crystal at resonance 14. The points connected by solid lines are the original data, while the dotted and dashed lines represent the  $\gamma$  rays believed to be present in the spectrum. The background is negligible over this portion of the spectrum, except for that arising from the nearby 873 keV resonance in the  $\text{F}^{19}(p,\alpha\gamma)\text{O}^{16}$  reaction.

The largest uncertainty in the determination of absolute yield,  $\omega\gamma$ , is perhaps the correction for the stopping power of the material. This is particularly true where the target material occurs as a compound and is prepared by evaporation in a thin layer. For this reason the absolute yields have been tabulated separately. They were calculated from the thick target yields from the stopping powers compiled by Allison and Warshaw<sup>15</sup> with the techniques discussed by Gove.<sup>14</sup>

The last column in Table II is a tabulation of the quantity  $(2J+1)\Gamma_\gamma$ . These have been calculated with the values of  $\Gamma_p/\Gamma$  given in reference 13 where known, otherwise, in general, with the assumption that  $\Gamma_p = \Gamma$ .

#### ACKNOWLEDGMENT

The authors wish to thank Mr. F. D. Lee for his assistance, both with taking the data and performing a number of the computations.

<sup>15</sup> S. K. Allison and S. D. Warshaw, *Revs. Modern Phys.* **25**, 779 (1953).